Targeting transforming growth factor-β2 by antisense oligodeoxynucleotide accelerates T cell-mediated tumor rejection in a humanized mouse model of triple-negative breast cancer

Hong Kyu Lee
Chungbuk National University
Hyeong-Jin Ji
Chungbuk National University
Sang-Kyung Shin
Chungbuk National University
Jihye Koo
Autotelic Bio
Tae Hun Kim
Autotelic Bio
Cho-Won Kim
Chungbuk National University
Yeon Hee Seong
Chungbuk National University
Jun-Eui Park
Autotelic Bio
Kyung-Chul Choi (kchoi@cbu.ac.kr)
Chungbuk National University College of Veterinary Medicine

Research

Keywords: TGF-β2 antisense, breast cancer, antitumor immunity, humanized model

Posted Date: April 5th, 2021

DOI: https://doi.org/10.21203/rs.3.rs-363729/v1

Version of Record: A version of this preprint was published at Cancer Immunology, Immunotherapy on January 31st, 2022. See the published version at https://doi.org/10.1007/s00262-022-03157-w.

Abstract

Background*:* Transforming growth factor (TGF-β) pathway mediates suppression of anti-tumor immunity, and is associated with poor prognosis in triple-negative breast cancer (TNBC).

Methods*:* In this study, we generated a humanized animal model by transplanting human peripheral blood mononuclear cells into immunodeficient mice followed by inoculation of MDA-MB-231 cells, and subsequently analyzed the role of TGF-β2 in the interaction between human T cells and human tumor cells.

Results*:* Following reconstitution of the human immune system, inhibition of TGF-β signaling by TGF-β2 antisense oligodeoxynucleotide (TASO) resulted in accelerated tumor growth inhibition. TGF-β2 inhibition also resulted in downregulation of peripheral Foxp3+ regulatory T cells (Treg), whereas no effect was seen in the expression of CD8+ cytotoxic T cells. Analysis of the TASO-treated mice serum revealed elevated levels of human **IFN-γ** and reduced levels of human IL-10 and TGF-β2. Moreover, TGF-β2 inhibition resulted in increased CD8+ T cell infiltration, whereas the reduced infiltration of Tregs into the tumor partly resulted from decreased expression of CCL22. Decreased intra-tumoral Tregs facilitated the activation of cytotoxic T cells, associated with increased granzyme B expression.

Conclusion*:* These results indicate that TASO potentiated T-cell mediated antitumor immunity, and it is proposed that TGF-β2 may be a promising target in the immunotherapeutic strategy of TNBC.

Background

Breast cancer is one of the most common cancer and the leading cause of cancer-related mortalities in women worldwide [1]. Triple-negative breast cancers (TNBCs) constitute approximately 10 - 20% of total breast cancers, and are characteristically lacking in the expressions of receptors for estrogen, progesterone, and human epidermal growth factor 2 [2, 3]. TNBC is the most aggressive subtype of breast cancer and the major cause of breast cancer related mortalities, due to high recurrence rate and drug resistance [4]. Although chemotherapies such as anthracycline, taxanes and eribulin are used in the early care of TNBC, to date there is no approved efficient standard treatment specifically targeted towards this subtype of breast cancer [5]. Various approaches for treating TNBC are currently underway, and therapies utilizing the host immune system are emerging as a promising treatment option.

The host immune system rejects most tumor cells through a multistep process called the cancer immunity cycle [6]. Although various types of immune cells are involved in the cancer immunity cycle, recognition and elimination of tumor cells are largely mediated by CD8+ cytotoxic T lymphocytes [7, 8]. However, tumors suppress the proliferation and functions of effector T cells by mediating cell to cell contact through immune checkpoint receptors [9, 10] and inducing the production of immunosuppressive factors including IL-10, indoleamine 2,3-dioxygenase, and transforming growth factor–beta (TGF-β) [11]. TGF-β released by tumor cells or their immunosuppressive microenvironments, such as tumor associated stroma and immune cells, is commonly enriched in TNBC and is related to poor prognosis [12].

The TGF-β cytokine superfamily comprises three isoforms (TGF-β1, β2, and β3) and other signaling proteins, which modulate numerous cellular functions such as proliferation, apoptosis, differentiation, and epithelial-mesenchymal transition (EMT) [13, 14]. Previous studies have demonstrated that TGF-β plays an important role in tumor initiation and progression. In the early stages of cancer, TGF-β inhibits cancer initiation by promoting cell cycle arrest and apoptosis, whereas cancer invasiveness and metastasis are promoted in the later stage of cancer [15, 16]. In addition, TGF-β mediates chemoresistance by regulating cancer stemness, EMT and autophagy [17-19]. Particularly, TGF-β suppresses anticancer immunity, enabling the cancer cells to escape immunosurveillance [20]. Of the three isoforms, most studies have intensively focused on TGF-β1, and a few studies have estimated the effects of TGF-β2 on antitumor immunity. These studies demonstrate that TGF-β2 mediates immunosuppressive effects through the inhibition of immune cell proliferation and activation [21, 22]. TGF-β2 also enables tumor cells to escape immunosurveillance by inhibiting tumor-infiltrating lymphocytes (TILs) [22] and downregulating the expression of HLA-DR in brain tumor [23]. As one of the most promising strategy for blockades of TGF-β signaling, TGF-β2 antisense oligodeoxynucleotide (TASO) has been clinically developed in some types of cancer such as malignant brain tumor, melanoma, and pancreatic cancer [24]. However, the specific mechanism of TGF-β2 on antitumor immunity is still elusive due to the limited research findings of TGF-β2 in immune-oncology field. Therefore, more comprehensive information on the role of TGF-β2 in antitumor immunity is required for translating tumor responses during clinical trials.

The current study undertook to investigate the antitumor effects of TGF-β2 inhibition by TASO in TNBC. In the tumor bearing humanized mouse model, we observed that blocking TGF-β2 potentiated the antitumor immunity by regulating CD8+ T cells and regulatory T cells (Tregs) at the tumor site as well as at the periphery. We believe this is the first *in vivo* study to demonstrate the effects of TGF-β2 inhibition on human T cell constituents, and its functional role at the tumor site. Our results indicate that blockade of TGF-β2 is considerably implicated in facilitation of immune surveillance, and their impact on antitumor immunity allows the advancement of TASO as a promising anticancer therapy.

Materials And Methods

Oligonucleotides and antibodies

TASO, also known as trabedersen, was provided by Autotelic Bio. Inc. (Cheongju, Korea). Antibodies used in flow cytometry analysis included PE-conjugated anti-human CD45 (clone 2D1), FITC-conjugated anti-human CD3 (clone HIT 3a), APC-conjugated anti-human CD8 (clone SK1), PE-conjugated anti-human CD4 (clone SK3), APC-conjugated anti-human CD25 (clone BC 96), and FITC-conjugated anti-human Foxp3 (clone 206D), and were procured from BioLegend (BioLegend, San Diego, CA, USA). Rabbit monoclonal antibodies against human CD8 (clone D8A8Y), Foxp3 (clone D2W8E), granzyme B (clone D6E9W), p-SMAD2/3 (clone D27F4), and rabbit polyclonal antibody against SMAD2/3 were purchased from Cell Signaling Technology (Cell Signaling Technology, Inc., Danvers, MA, USA). Rabbit polyclonal antibody against human TGF-β2, CCL-22 and horseradish peroxidase (HRP)-conjugated goat polyclonal antibody

to rabbit IgG were purchased from Abcam (Abcam, Cambridge, UK). Mouse monoclonal antibody against β-actin and HRP-conjugated goat polyclonal antibody to mouse IgG were obtained from Santa Cruz Biotechnology (Santa Cruz Biotechnology, Santa Cruz, CA, USA).

Animals

Four-week old female NOD/scid/IL-2Rγ$^{-/-}$ (NOD.Cg-Prkdc^{scid}Il2rg^{tm1Wjl}/SzJ, NSG) mice were purchased from Charles River Japan, and acclimated for 1 week. All procedures involving experimental animals complied with regulations for the care and use of laboratory animals of the animal ethics committee of Chungbuk National University (CBNUA-1235-18-01). The mice were maintained under specific pathogen free conditions, according to guidelines of the National Institutes of Health for the care and use of laboratory animals.

Preparation and transplantation of human peripheral blood mononuclear cells (PBMCs)

The human cryopreserved PBMCs obtained from Zen-Bio (Zen-Bio, INC., Research Triangle, NC, USA) were quickly **thawed and washed once. Human PBMCs used in this study were isolated from a healthy single donor,** the information of PBMCs such as HLA types, viability and population distribution was provided by Zen-Bio (Zen-Bio, INC., Research Triangle, NC, USA)**. PBMCs were incubated in the lymphocyte specific RPMI1640 medium supplemented with 20% FBS and DNAse I (LYMPH-1;** Zen-Bio, INC., Research Triangle, NC, USA**) for 1h;** 1×10^7 cells were subsequently resuspended in PBS and injected into the lateral side of tail vein of mice. Preliminary experiment was performed to evaluate appearance of human PBMCs in mouse blood and onsets of graft versus host disease (GvHD).

Establishment of xenografts

The MDA-MB-231 TNBC cell line procured from the American Type Culture Collection was cultured in RPMI1640 supplemented with 10% FBS, 100 IU/ml penicillin, and 100 µg/ml streptomycin, in a humidified chamber with 5% CO_2 at 37°C. A total of 1×10^7 MDA-MB-231 tumor cells suspended in PBS were implanted subcutaneously in the right flanks of NSG mice (this is day 0 of the experiment), 6 days after human PBMC engraftment. Mice were intra-peritoneally administered with TASO every alternate day, starting from day 3. From day 4, tumor volume was measured every alternate day using a caliper, and calculated using the formula (length) × (width)^2/2**.** Mice were sacrificed on day 19, and the implanted tumors were harvested, weighed, and processed for analysis **(Fig. 2A)**.

Fluorescence activated cell sorting (FACS)

Using a capillary tube, mouse blood was collected from the orbital venous plexus into an EDTA tube on days 17 and 19. RBCs were eliminated by incubating 100 µl blood with RBC lysis buffer (BioLegend, San Diego, CA, USA), after which the cells were washed with cell staining buffer (BioLegend, San Diego, CA, USA). Washed cells were subsequently incubated with anti-CD16/32 for 5 min at 4°C, to block the Fc receptors and reduce non-specific binding. On day 17, cells were subjected to PE-conjugated anti-human

CD4, APC-conjugated anti-human CD25 for cell surface staining, and FITC-conjugated anti-human Foxp3 for intracellular staining, after fixing/permeabilization with True-Nuclear™ Transcription factor buffer set (BioLegend, San Diego, CA, USA). And PE-conjugated anti-human CD45, FITC-conjugated anti-human CD3, and APC-conjugated anti-human CD8 were used for cell surface staining on day 19. Staining with antibodies was performed for 30 min at 4℃ in the dark. Stained cells were washed with cell staining buffer, followed by 4% paraformaldehyde fixation. The fluorescence of stained cells was measured by FACS Aria II (BD Bioscience, San Diego, CA, USA), and data were analyzed using the FlowJo software (TreeStar, San Carlos, CA, USA).

Cytokine measurement

Mouse blood was collected from the caudal vena cava on day 19, and serum was isolated for cytokine analysis. Levels of human IL-10, **IFN-γ**, and TGF-β2 in mouse serum were measured by applying the human magnetic luminex assay kit (R&D systems, Abingdon, UK), according to the manufacturer's instruction. Measurement was performed on the Luminex 200™ (Luminex, Austain, TX, USA), and analyzed using the Masterplex QT 2010 Software (MiraiBio, Hitachi, CA, USA).

Immunohistochemistry (IHC)

Paraffin-embedded spleen and implanted tumors were cut into 4 μm thick sections, deparaffinized, and subsequently rehydrated. After rehydration, antigen retrieval was performed by incubating with 10 mM sodium citrate buffer (pH 6.0) at 100℃ for 10 min. The tissue sections were then incubated with 3% hydrogen peroxide in PBS to block the endogenous peroxidase activity, followed by incubation with 5% BSA in PBS to reduce non-specific binding. The slides were subsequently incubated overnight with primary antibodies against human TGF-β2 (1:100), CCL22 (1:200), Foxp3 (1:200), CD8 (1:200), and granzyme B (1:200). The slides were subsequently incubated with a biotinylated secondary antibody for 1 h, and signals were amplified by avidin-biotin peroxidase complexes (ABC Elite kit; Vector Labs, Burlingame, CA, USA) for 30 min. Peroxidase activity was visualized using the DAB kit (Vector Labs, Burlingame, CA, USA), followed by counterstaining with hematoxylin. Images were captured with Axio Imager A2 microscope (Carl Zeiss, Jena, Germany) and DAB intensity was semi-quantified using Image J Fiji software (version 1.53c; WS Rasband, National Institute of Health, Bathesda, MD, USA) as described previously [25].

Western blotting

After sacrifice on day 19, tumor tissues were harvested and homogenized with pro-prep buffer (iNtRON Biotechnology, Inc., Seongnam, Korea) to extract the total proteins. Protein concentration was measured by the modified Bradford method, using the pro-measure kit (iNtRON Biotechnology, Inc., Seongnam, Korea) at 595 nm. Approximately 40 μg of total protein was loaded and resolved on 12.5% SDS-PAGE, followed by transferring to a PVDF membrane (Perkin Elmer Co., Waltham, MA, USA). The membrane was subsequently incubated with rabbit monoclonal antibodies against p-SMAD 2/3, SMAD 2/3 (1:1000) and mouse monoclonal antibody against β-actin (1:2000), followed by HRP conjugated secondary antibodies

against anti-rabbit or anti-mouse (1:3000). Immunoreactive bands were detected using a chemiluminescent detection reagent (Thermo Fisher Scientific Inc., Waltham, MA USA), which is an HRP chemiluminescent substrate. The luminescence intensity of the target protein bands was detected using the Lumino Graph 2 (ATTO Corporation, Tokyo, Japan), and adjusted by the Image Saver 6 (ATTO Corporation, Tokyo, Japan). Intensity levels of images were quantified using Image J analysis software (version 1.53e; WS Rasband, National Institute of Health, Batheda, MD, USA).

Statistical analysis

All data are presented as means ± standard errors of the mean (S.E.M.), and statistical significance was analyzed by one-way analysis of variance (ANOVA) followed by a *post hoc* Dunnett's test using the GraphPad Prism 5.01 software (GraphPad Software Inc., San Diego, CA, USA). A p-value < 0.05 is considered statistically significant.

Results

Generation of human CD3+ T cell dominant humanized mouse model

To determine the human T cell-mediated antitumor immune response by TGF-β2 inhibition, we generated tumor bearing humanized mice (huPBL NSG mouse) by engrafting human PBMC and subcutaneously inoculating MDA-MB-231 cells into NSG mice. Since the significance of HLA matching between PBMC donor and MDA-MB-231 cells (HLA-A2+ cell line) were checked in advance (data not shown), HLA-A2 positive human PBMC from a single donor was used in this study. The persistence of human T cells in the peripheral blood of huPBL NSG mice was determined by FACS on days 7 and 25 after human PBMC transplantation by the gating protocol described previously [26]. The increased human CD45+ cells in mouse blood were observed on day 25 after human PBMC transplantation (Fig. 1A and B). As shown in Fig. 1A and C, the human CD45+CD3+ cells, which represent human T lymphocytes, were markedly increased 25 days after human PBMC engraftment. Moreover, an increase in the proportion of human CD8+ cells among the human CD3+ T cells was observed on day 25 following humanization (Fig. 1C and D). These results confirm establishment of the human CD3+ T lymphocyte dominant humanized animal model following transplantation of human PBMC.

TASO administration accelerates tumor rejection in huPBL NSG mice

Previous studies have demonstrated that reconstitution of the immune system by transplanting human PBMC hampers tumor growth in immunocompromised mice [27, 28]. In this study, tumor volume was measured every alternate day, from day 4 after tumor inoculation. We observed a significant decrease in the tumor volume from day 12 in the group transplanted with human PBMC, as compared to the tumor only group (Fig. 2B). Additionally, from day 10 onwards, the human PBMC engrafted group with TASO administration showed significantly decreased tumor volumes, compared to the PBMC + vehicle group (Fig. 2B and Table 1).

We further evaluated tumor weights after the mice were sacrificed. In agreement with the data of tumor volume, tumor weights of the PBMC engrafted group were notably lesser than tumor weights of the tumor only group. The human PBMC transplanted and TASO (32 mg/kg) treated groups showed extreme tumor regression on day 19 (Fig. 2C). Representative photos of tumor from tumor only-, PBMC + vehicle -, and PBMC + TASO-treated groups are presented in Fig. 2D.

TASO administration mediates TGF-β2 inhibition, and is associated with decreased TGF-β signaling

Tumoral TGF-β2 protein expression patterns were evaluated by IHC to confirm the effect of TASO-induced TGF-β2 inhibition. As shown in Fig. 3A and B, TGF-β2 expressions were decreased in the TASO (16 mg/kg and 32 mg/kg) treated group, as compared to the PBMC + vehicle group.

The tumoral expression levels of phosphorylated SMAD2/3 (p-SMAD 2/3) and SMAD2/3 (the main downstream effector proteins of TGF-β signaling) were evaluated by western blot. As shown in Fig. 3C, expression levels of p-SMAD2/3 were decreased in the TASO-treated tumors, as compared to the untreated group. In particular, the relative ratio of p-SMAD2/3 levels to SMAD2/3 levels was significantly decreased in PBMC + TASO (32 mg/kg) group compared to PBMC + vehicle group (Fig. 3D). We therefore conclude that the expression level of p-SMAD2/3 in tumors is positively correlated with TGF-β2 expression.

TGF-β2 inhibition modifies the subpopulation of human CD8+ T cells and Tregs in the peripheral blood and spleen of huPBL NSG mice

Since antitumor immune response is associated with alteration of the T cell immune constitution, we examined recruitment of human Tregs and CD8+ T cells in the peripheral blood and spleen. Because human PBMCs were not transplanted into the tumor only group, no human Foxp3+ cells were observed in the peripheral blood and spleen of tumor only group. In the FACS analysis, the proportion of human CD25+Foxp3+ cells (of the human CD4+ cells in peripheral blood) were significantly decreased after exposure to TASO (16 mg/kg and 32 mg/kg) (Fig. 4A and B). IHC staining showed significant decrease in the population of splenic human Foxp3+ cells after TASO administration (Fig. 5A and B).

While human CD8+ cells were not observed in peripheral blood and spleen of the tumor only group, numerous CD8+ cells appeared in the peripheral blood and spleen of the human PBMC engrafted groups. FACS analysis revealed no difference in the proportion of human CD3+CD8+ cells (belonging to the human CD45+ cells) in the peripheral blood and spleen, between the PBMC + vehicle and PBMC + TASO treated groups (Fig. 4A and C). In addition, IHC staining also revealed no significant difference in the number of human CD8+ cytotoxic T cells in the spleen of PBMC + TASO treated and PBMC + vehicle groups (Fig. 5A and C).

TGF-β2 inhibition alters the human cytokine levels in huPBL NSG mice

Since alterations in the T cell subpopulation modify immune responses, serum levels of cytokines such as TGF-β2, IL-10 and IFN-γ were measured after mice were sacrificed. The main source of serum TGF-β2

is tumor tissues and human T cells; hence, decreased serum TGF-β2 levels in the human PBMC engrafted group could partly be affected by tumor size. Additionally, in animals administered TASO (32 mg/kg), the serum levels of TGF-β2 were markedly decreased, compared to the PBMC + vehicle group (Fig. 6A).

IL-10 is an immune-suppressive cytokine that is mainly released by Tregs, while IFN-γ is an immune-activating cytokine released by T cells (including T helper cells and cytotoxic T cells) [29, 30]. Human IL-10 and IFN-γ were not detected in the tumor only group since there was no grafting of human PBMCs. Serum human IL-10 level was significantly increased in the PBMC engrafted animals, when compared to the tumor only group. However, administration of TASO (32 mg/kg) significantly reduced the levels of human IL-10 (Fig. 6B). We also observed that PBMC engraftment increases the human IFN-γ level when compared to the tumor only group, and TASO administration (16 and 32 mg/kg) significantly augmented human IFN-γ production (Fig. 6C).

TGF-β2 inhibition regulates activation and infiltration of T lymphocytes into the tumor

Alteration of the immune status, including immune cell composition and cytokine levels, modifies the activation and infiltration of lymphocytes at the tumor site [29]. We therefore examined the change in numbers of Foxp3+ cells and CD8+ T cells in tumor tissues at day 25 after human PBMC engraftment. Because CCL22 expression in tumor positively correlates with infiltration of Tregs [31, 32], we examined the CCL22 expression in tumor tissues by IHC. As shown in Fig. 7A and B, decreased CCL22 expression was determined in the PBMC + TASO treated group, as compared to the PBMC + vehicle treated group. Moreover, human Foxp3+ cells were not detected in the tumor only group, but several Foxp3+ cells were detected in the tumor tissues of PBMC + vehicle treated group, and the infiltration of human Foxp3+ cells into the tumor was hampered by TASO administration (Fig. 7A and C).

Human CD8+ cells were not observed in the tumor tissues of tumor only group, but numerous human CD8+ cells were observed to infiltrate the tumor tissues of the human PBMC engrafted groups. Particularly, a greater number of human CD8+ cytotoxic T cells were observed in tumor tissues of the PBMC + TASO treated group, as compared to the PBMC + vehicle treated group (Fig. 7A and D). TASO treatment facilitated the widespread disbursal of CD8+ cytotoxic T cells throughout entire tumors, including center of the tumors. Since granzyme B expression is positively correlated with activation of CD8+ mediated antitumor activity, we applied IHC to evaluate granzyme B expressrion levels in the tumor tissues. As shown in Fig. 7A and E, granzyme B expression was increased in tumor tissues of the PBMC + TASO treated groups, as compared to the PBMC + vehicle treated group. Therefore, our results indicate that TASO treatment possibly modifies the distribution and functional capacity of CD8+ cytotoxic T cells, thereby exerting antitumor immunity towards tumor tissues.

Discussion

TASO is complementary to specific 18-nucleotide sequences of the human TGF-β2 mRNA, and are known to interrupt TGF-β signaling by inhibiting TGF-β2 protein synthesis [33]. In this study, TGF-β2 expression was significantly reduced after exposure to TASO, and blockade of TGF-β2 by TASO subsequently

downregulated the TGF-β/SMAD pathway in MDA-MB-231 tumors. In fact, TGF-β/SMAD signaling is mainly dependent on TGF-β1 due to its higher affinity to TGF-β receptor II and greater amounts than other TGF-β isoforms in breast cancer [34, 35]. Since it is well documented that TGF-β isoforms exhibit auto- and cross regulatory actions [33], the inhibition of TGF-β/SMAD signaling by TASO might result not only by direct decrease of TGF-β2, but also indirect downregulation of TGF-β1.

TGF-β is a pleiotropic cytokine released from various cells such as immune cells, stromal cells and tumor cells in the tumor microenvironment, and is associated with poor prognosis in multiple tumors including breast cancer, melanoma, and pancreatic cancer [12, 36, 37]. The tumor promoting effects of TGF-β not only result from direct intrinsic effects on tumor cells, but are also derived from indirect extrinsic effects on the tumor microenvironment [38, 39]. Especially, TGF-β plays a crucial role in immunosuppression via modulation of Tregs [40, 41]. It is well known that Tregs mediate the immunological tolerance to tumor cells by producing inhibitory cytokines and downregulating effector T cells [42]. Since Tregs are considered a major problem in antitumor immunity, numerous studies have focused on the correlation between anti-TGF-β therapy and inhibition of Tregs [43, 44]. Although TGF-β signaling is closely related with Treg differentiation by inducing Foxp3 expression, previous *in vivo* studies did not present consistent results of diminished Tregs population by TGF-β inhibition [8, 44]. These studies investigated the effect of the TGF-β antibody on mouse Tregs by using the transgenic mouse model or syngeneic mouse tumor model. In the present study, we confirmed that the human Tregs population is downregulated by inhibiting TGF-β2 production in the huPBL NSG model, indicating that TGF-β2 plays a specific role in differentiation of Tregs during the immune reconstitution process. Tregs not only produce a number of anti-inflammatory cytokines (including TGF-β, IL-10, and IL-35) [45, 46], but also induce other cells to produce inhibitory cytokines [47]. Cytokines are released from various cells in the cancer microenvironment, and a balance between anti-inflammatory and pro-inflammatory cytokines regulates the activation of T cells, followed by apoptosis of tumor cells [29]. IL-10 produced by immune cells such as macrophages, T cells, and natural killer cells promotes tumor cell proliferation and invasiveness via immunosuppressive effects [30, 48]. **IFN-γ** produced predominantly by T cells and NK cells decreases the tumor cell growth by direct inhibitory effects of tumor cell proliferation, as well as indirect immune stimulating effects [29]. The current results indicate that blockade of TGF-β2 induces a significant increase of human **IFN-γ** and decrease of human IL-10 in humanized mouse serum. These results imply that an altered balance of cytokines by TGF-β2 inhibition might partly contribute to the downregulation of Tregs, resulting in enhancing T cell-mediated tumor rejection.

Based on their immunological properties, solid tumors are commonly divided into three categories: immune inflamed, immune excluded, and immune desert [8, 49]. TILs play an important role in determining the antitumor immunity, and their frequency is commonly lowest in immune desert tumors, intermediate in immune excluded tumors, and highest in immune inflamed tumors [49]. While increased infiltration of Tregs in a tumor is associated with poor prognosis, the increased infiltration of CD8+ cytotoxic T cells in tumors is inversely connected to a poor prognosis in many cancers [50, 51]. Since TGF-β inhibition converts tumor phenotypes from immune excluded to immune inflamed mediating anti-tumor immune responses [8], blockade of TGF-β2 also mediates a significant increase in the abundance

of CD8+ cytotoxic T cells. It has been demonstrated that TGF-β and CCL22 are possible chemoattractants for intratumoral infiltration of Tregs [31, 32], and activated TGF-β pathway facilitates intratumoral production of CCL22 [52, 53]. The current study results showing decreased TGF-β signaling and CCL22 secretion in tumors subsequent to TASO administration, is possibly correlated with downregulation of intratumoral Tregs infiltration. While previous studies on anti-TGF-β therapies were performed in immune excluded tumor models [8], the current study applied TGF-β2 inhibition in the immune inflamed TNBC bearing huPBL model, to compare the alteration of CD8+ infiltration as well as Foxp3+Treg infiltration throughout the entire tumor. Since TILs in immune inflamed tumors (such as TNBCs) contain a relatively high frequency of CD8+ cytotoxic T cells as well as Tregs, the ratio of Tregs to cytotoxic T cells in the tumor site mainly determines the success of antitumor immunity [54]. Therefore, a decreased ratio of Tregs to cytotoxic T cells due to TGF-β2 inhibition might be associated with augmentation of cytotoxic T cell-mediated tumor regression. Granzyme B is commonly secreted by cytotoxic T cells and NK cells mediating apoptosis of tumor cells [55]. Consistent with a previous study [20], blockade of TGF-β2 induced increased granzyme B expression in the current study, which was inversely associated with TGF-β signaling in the tumor tissue. These results indicate that TGF-β2 inhibition enhances T cell-mediated antitumor immunity by appropriate arrangement of T cell subpopulation and activation of cytotoxic T cells in tumor tissues, resulting in tumor regression.

In this study, we established a humanized model by transplanting human PBMCs into immunocompromised mice, followed by implantation of the human TNBC cell line. The huPBL NSG model is a simple and economic humanized model providing an appropriate research platform to investigate the reciprocal interaction between human T cells and human cancer cells [56]. In this humanized model, reconstituted human PBMCs are human CD3+ T cell dominant, and mimic the pattern of human TILs, such as trafficking, infiltration and activation, within tumor microenvironment. Similar to other studies [27, 28], we confirmed that transplantation of human PBMCs results in reduced tumor growth, accompanied by human CD8+ T cells in tumoral and peripheral sites. Despite the advantage of this model, several potential limitations still exist. Although we used HLA-A2 matched PBMCs with MDA-MB-231 cells, it is not possible to completely adjust all other characteristics of the isolated PBMCs. Transplanting PBMCs and tumors from the same patient into immune deficient mouse might be one of the prospective approaches to generate a completely autologous humanized model. In addition, the therapeutic time window in a huPBL NSG platform is restricted to less than 6 weeks after PBMC engraftment due to development of GvHD. Although an alternative humanized model reconstituted with human CD34+ hematopoietic stem cells is available without GvHD, there are still challenges such as HLA mismatch with tumor, high cost, and a longer time for reconstitution [56]. Therefore, a more novel preclinical model is required to break through the existing challenges in immuno-oncology research.

Conclusions

The inhibition of TGF-β2 protein production with TASO induces antitumor immunity via downregulation of Tregs and upregulation of cytotoxic T cells at the periphery and/or within the tumor. Although anti-TGF-β mono-therapies have shown incomplete anticancer effects in numerous clinical studies due to its

limited activity on anti-proliferation or apoptosis, it is likely that TASO exhibits attractive potential in combination with other therapies, such as immune checkpoint inhibitors or immune-stimulators.

Abbreviations

CCL22: C-C Motif Chemokine Ligand 22; CD4: Cluster of Differentiation 4; CD8: Cluster of Differentiation 8; CD16/32: Cluster of Differentiation 16/32; CD25: Cluster of Differentiation 25; CD34: Cluster of Differentiation 34; CD45: Cluster of Differentiation 45; CTLs: Cytotoxic T Lymphocytes; DAB: Dimethylaminoazobenzene; Foxp3: Forkhead box P3; GvHD: Graft-versus-Host Disease HLA: Human Leukocyte Antigen; IFN-γ: Interferon-gamma; NSG: NOD.Cg-Prkdc^{scid}Il2rg^{tm1Wjl}/SzJ; TASO: TGF-β2 Antisense Oligodeoxynucleotide; TGF-β: Transforming Growth Factor-beta; TNBC: Triple-Negative Breast Cancer; Tregs: regulatory T cells

Declarations

Ethics approval and consent to participate

All procedures involving experimental animals complied with regulations for the care and use of laboratory animals of the animal ethics committee of Chungbuk National University (CBNUA-1235-18-01).

Consent for publication

All authors have agreed to consent these data for publication.

Availability of data and material

The data and materials are available following publication of this paper.

Competing interests

Jun-Eui Park, Jihye Koo, and Tae Hun Kim are current employees of Autotelic Bio, Inc. All other authors do not have any conflicts of interest to declare.

Funding

This work was supported by the Tech Incubator Program for Startup (S2645586) through Chungbuk Center for Creative Economy & Innovation funded by Ministry of Small and Medium Enterprises and Startups (MSS). In addition, this work was also supported by the Basic Science Research Program through the National Research Foundation (NRF) of Korea funded by the Ministry of Science and ICT (2020R1A2C2006060).

Authors' contributions

K.C.C. and J.E.P. conceived an idea of the manuscript. H.K.L, H.J.J., S.K.S. and C.W.K. performed the experiment and statistical analysis. H.K.L. made the first draft of the manuscript and Y.H.S., J.E.P. and K.C.C. edited and revised the manuscript based on the concept. T.H.K., J.K., J.E.P. and K.C.C. provided some materials and essential techniques for this study.

Acknowledgements

N/A

References

1. Siegel RL, Miller KD, Jemal A: **Cancer statistics, 2019**. *CA Cancer J Clin* 2019, **69**(1):7-34.
2. Denkert C, Liedtke C, Tutt A, von Minckwitz G: **Molecular alterations in triple-negative breast cancer-the road to new treatment strategies**. *Lancet* 2017, **389**(10087):2430-2442.
3. Lehmann BD, Bauer JA, Chen X, Sanders ME, Chakravarthy AB, Shyr Y, Pietenpol JA: **Identification of human triple-negative breast cancer subtypes and preclinical models for selection of targeted therapies**. *J Clin Invest* 2011, **121**(7):2750-2767.
4. Dent R, Trudeau M, Pritchard KI, Hanna WM, Kahn HK, Sawka CA, Lickley LA, Rawlinson E, Sun P, Narod SA: **Triple-negative breast cancer: clinical features and patterns of recurrence**. *Clin Cancer Res* 2007, **13**(15 Pt 1):4429-4434.
5. Diana A, Carlino F, Franzese E, Oikonomidou O, Criscitiello C, De Vita F, Ciardiello F, Orditura M: **Early Triple Negative Breast Cancer: Conventional Treatment and Emerging Therapeutic Landscapes**. *Cancers (Basel)* 2020, **12**(4).
6. Chen DS, Mellman I: **Oncology meets immunology: the cancer-immunity cycle**. *Immunity* 2013, **39**(1):1-10.
7. Horton BL, Williams JB, Cabanov A, Spranger S, Gajewski TF: **Intratumoral CD8(+) T-cell Apoptosis Is a Major Component of T-cell Dysfunction and Impedes Antitumor Immunity**. *Cancer Immunol Res* 2018, **6**(1):14-24.
8. Mariathasan S, Turley SJ, Nickles D, Castiglioni A, Yuen K, Wang Y, Kadel EE, III, Koeppen H, Astarita JL, Cubas R *et al*: **TGFbeta attenuates tumour response to PD-L1 blockade by contributing to exclusion of T cells**. *Nature* 2018, **554**(7693):544-548.
9. Dong H, Strome SE, Salomao DR, Tamura H, Hirano F, Flies DB, Roche PC, Lu J, Zhu G, Tamada K *et al*: **Tumor-associated B7-H1 promotes T-cell apoptosis: a potential mechanism of immune evasion**. *Nat Med* 2002, **8**(8):793-800.
10. Freeman GJ, Long AJ, Iwai Y, Bourque K, Chernova T, Nishimura H, Fitz LJ, Malenkovich N, Okazaki T, Byrne MC *et al*: **Engagement of the PD-1 immunoinhibitory receptor by a novel B7 family member leads to negative regulation of lymphocyte activation**. *J Exp Med* 2000, **192**(7):1027-1034.
11. Bates JP, Derakhshandeh R, Jones L, Webb TJ: **Mechanisms of immune evasion in breast cancer**. *BMC Cancer* 2018, **18**(1):556.

12. Bahhnassy A, Mohanad M, Shaarawy S, Ismail MF, El-Bastawisy A, Ashmawy AM, Zekri AR: **Transforming growth factor-beta, insulin-like growth factor I/insulin-like growth factor I receptor and vascular endothelial growth factor-A: prognostic and predictive markers in triple-negative and non-triple-negative breast cancer**. *Mol Med Rep* 2015, **12**(1):851-864.
13. Moustakas A, Pardali K, Gaal A, Heldin CH: **Mechanisms of TGF-beta signaling in regulation of cell growth and differentiation**. *Immunol Lett* 2002, **82**(1-2):85-91.
14. Xu J, Lamouille S, Derynck R: **TGF-beta-induced epithelial to mesenchymal transition**. *Cell Res* 2009, **19**(2):156-172.
15. Derynck R, Akhurst RJ, Balmain A: **TGF-beta signaling in tumor suppression and cancer progression**. *Nat Genet* 2001, **29**(2):117-129.
16. Lebrun JJ: **The Dual Role of TGFbeta in Human Cancer: From Tumor Suppression to Cancer Metastasis**. *ISRN Mol Biol* 2012, **2012**:381428.
17. Bruna A, Greenwood W, Le Quesne J, Teschendorff A, Miranda-Saavedra D, Rueda OM, Sandoval JL, Vidakovic AT, Saadi A, Pharoah P *et al*: **TGFbeta induces the formation of tumour-initiating cells in claudinlow breast cancer**. *Nat Commun* 2012, **3**:1055.
18. Kiyono K, Suzuki HI, Matsuyama H, Morishita Y, Komuro A, Kano MR, Sugimoto K, Miyazono K: **Autophagy is activated by TGF-beta and potentiates TGF-beta-mediated growth inhibition in human hepatocellular carcinoma cells**. *Cancer Res* 2009, **69**(23):8844-8852.
19. Xu X, Zhang L, He X, Zhang P, Sun C, Xu X, Lu Y, Li F: **TGF-beta plays a vital role in triple-negative breast cancer (TNBC) drug-resistance through regulating stemness, EMT and apoptosis**. *Biochem Biophys Res Commun* 2018, **502**(1):160-165.
20. Thomas DA, Massague J: **TGF-beta directly targets cytotoxic T cell functions during tumor evasion of immune surveillance**. *Cancer Cell* 2005, **8**(5):369-380.
21. Kuppner MC, Hamou MF, Bodmer S, Fontana A, de Tribolet N: **The glioblastoma-derived T-cell suppressor factor/transforming growth factor beta 2 inhibits the generation of lymphokine-activated killer (LAK) cells**. *Int J Cancer* 1988, **42**(4):562-567.
22. Kuppner MC, Hamou MF, Sawamura Y, Bodmer S, de Tribolet N: **Inhibition of lymphocyte function by glioblastoma-derived transforming growth factor beta 2**. *J Neurosurg* 1989, **71**(2):211-217.
23. Zuber P, Kuppner MC, De Tribolet N: **Transforming growth factor-beta 2 down-regulates HLA-DR antigen expression on human malignant glioma cells**. *Eur J Immunol* 1988, **18**(10):1623-1626.
24. Vallieres L: **Trabedersen, a TGFbeta2-specific antisense oligonucleotide for the treatment of malignant gliomas and other tumors overexpressing TGFbeta2**. *IDrugs : the investigational drugs journal* 2009, **12**(7):445-453.
25. Crowe AR, Yue W: **Semi-quantitative Determination of Protein Expression using Immunohistochemistry Staining and Analysis: An Integrated Protocol**. *Bio-protocol* 2019, **9**(24).
26. Pyo KH, Kim JH, Lee JM, Kim SE, Cho JS, Lim SM, Cho BC: **Promising preclinical platform for evaluation of immuno-oncology drugs using Hu-PBL-NSG lung cancer models**. *Lung cancer* 2019, **127**:112-121.

27. Liu X, Li H, Liu J, Guan Y, Huang L, Tang H, He J: **Immune reconstitution from peripheral blood mononuclear cells inhibits lung carcinoma growth in NOD/SCID mice**. *Oncol Lett* 2014, **8**(4):1638-1644.
28. Roth MD, Harui A: **Human tumor infiltrating lymphocytes cooperatively regulate prostate tumor growth in a humanized mouse model**. *J Immunother Cancer* 2015, **3**:12.
29. Burkholder B, Huang RY, Burgess R, Luo S, Jones VS, Zhang W, Lv ZQ, Gao CY, Wang BL, Zhang YM *et al*: **Tumor-induced perturbations of cytokines and immune cell networks**. *Biochim Biophys Acta* 2014, **1845**(2):182-201.
30. Jarnicki AG, Lysaght J, Todryk S, Mills KH: **Suppression of antitumor immunity by IL-10 and TGF-beta-producing T cells infiltrating the growing tumor: influence of tumor environment on the induction of CD4+ and CD8+ regulatory T cells**. *J Immunol* 2006, **177**(2):896-904.
31. Li YQ, Liu FF, Zhang XM, Guo XJ, Ren MJ, Fu L: **Tumor secretion of CCL22 activates intratumoral Treg infiltration and is independent prognostic predictor of breast cancer**. *PLoS One* 2013, **8**(10):e76379.
32. Mizukami Y, Kono K, Kawaguchi Y, Akaike H, Kamimura K, Sugai H, Fujii H: **CCL17 and CCL22 chemokines within tumor microenvironment are related to accumulation of Foxp3+ regulatory T cells in gastric cancer**. *Int J Cancer* 2008, **122**(10):2286-2293.
33. Jaschinski F, Rothhammer T, Jachimczak P, Seitz C, Schneider A, Schlingensiepen KH: **The antisense oligonucleotide trabedersen (AP 12009) for the targeted inhibition of TGF-beta2**. *Curr Pharm Biotechnol* 2011, **12**(12):2203-2213.
34. Hachim MY, Hachim IY, Dai M, Ali S, Lebrun JJ: **Differential expression of TGFbeta isoforms in breast cancer highlights different roles during breast cancer progression**. *Tumour Biol* 2018, **40**(1):1010428317748254.
35. Qian SW, Burmester JK, Tsang ML, Weatherbee JA, Hinck AP, Ohlsen DJ, Sporn MB, Roberts AB: **Binding affinity of transforming growth factor-beta for its type II receptor is determined by the C-terminal region of the molecule**. *J Biol Chem* 1996, **271**(48):30656-30662.
36. Javle M, Li Y, Tan D, Dong X, Chang P, Kar S, Li D: **Biomarkers of TGF-beta signaling pathway and prognosis of pancreatic cancer**. *PLoS One* 2014, **9**(1):e85942.
37. Tas F, Karabulut S, Yasasever CT, Duranyildiz D: **Serum transforming growth factor-beta 1 (TGF-beta1) levels have diagnostic, predictive, and possible prognostic roles in patients with melanoma**. *Tumour Biol* 2014, **35**(7):7233-7237.
38. Tauriello DVF, Palomo-Ponce S, Stork D, Berenguer-Llergo A, Badia-Ramentol J, Iglesias M, Sevillano M, Ibiza S, Canellas A, Hernando-Momblona X *et al*: **TGFbeta drives immune evasion in genetically reconstituted colon cancer metastasis**. *Nature* 2018, **554**(7693):538-543.
39. Yu Y, Xiao CH, Tan LD, Wang QS, Li XQ, Feng YM: **Cancer-associated fibroblasts induce epithelial-mesenchymal transition of breast cancer cells through paracrine TGF-beta signalling**. *Br J Cancer* 2014, **110**(3):724-732.

40. Chen W, Jin W, Hardegen N, Lei KJ, Li L, Marinos N, McGrady G, Wahl SM: **Conversion of peripheral CD4+CD25- naive T cells to CD4+CD25+ regulatory T cells by TGF-beta induction of transcription factor Foxp3**. *J Exp Med* 2003, **198**(12):1875-1886.
41. Shen Y, Wei Y, Wang Z, Jing Y, He H, Yuan J, Li R, Zhao Q, Wei L, Yang T *et al*: **TGF-beta regulates hepatocellular carcinoma progression by inducing Treg cell polarization**. *Cell Physiol Biochem* 2015, **35**(4):1623-1632.
42. Wu H, Li P, Shao N, Ma J, Ji M, Sun X, Ma D, Ji C: **Aberrant expression of Treg-associated cytokine IL-35 along with IL-10 and TGF-beta in acute myeloid leukemia**. *Oncol Lett* 2012, **3**(5):1119-1123.
43. Polanczyk MJ, Walker E, Haley D, Guerrouahen BS, Akporiaye ET: **Blockade of TGF-beta signaling to enhance the antitumor response is accompanied by dysregulation of the functional activity of CD4(+)CD25(+)Foxp3(+) and CD4(+)CD25(-)Foxp3(+) T cells**. *J Transl Med* 2019, **17**(1):219.
44. Pu N, Zhao G, Yin H, Li JA, Nuerxiati A, Wang D, Xu X, Kuang T, Jin D, Lou W *et al*: **CD25 and TGF-beta blockade based on predictive integrated immune ratio inhibits tumor growth in pancreatic cancer**. *J Transl Med* 2018, **16**(1):294.
45. Annacker O, Asseman C, Read S, Powrie F: **Interleukin-10 in the regulation of T cell-induced colitis**. *J Autoimmun* 2003, **20**(4):277-279.
46. Collison LW, Workman CJ, Kuo TT, Boyd K, Wang Y, Vignali KM, Cross R, Sehy D, Blumberg RS, Vignali DA: **The inhibitory cytokine IL-35 contributes to regulatory T-cell function**. *Nature* 2007, **450**(7169):566-569.
47. Kearley J, Barker JE, Robinson DS, Lloyd CM: **Resolution of airway inflammation and hyperreactivity after in vivo transfer of CD4+CD25+ regulatory T cells is interleukin 10 dependent**. *J Exp Med* 2005, **202**(11):1539-1547.
48. Rong L, Li R, Li S, Luo R: **Immunosuppression of breast cancer cells mediated by transforming growth factor-beta in exosomes from cancer cells**. *Oncol Lett* 2016, **11**(1):500-504.
49. Kather JN, Suarez-Carmona M, Charoentong P, Weis CA, Hirsch D, Bankhead P, Horning M, Ferber D, Kel I, Herpel E *et al*: **Topography of cancer-associated immune cells in human solid tumors**. *Elife* 2018, **7**.
50. Sato E, Olson SH, Ahn J, Bundy B, Nishikawa H, Qian F, Jungbluth AA, Frosina D, Gnjatic S, Ambrosone C *et al*: **Intraepithelial CD8+ tumor-infiltrating lymphocytes and a high CD8+/regulatory T cell ratio are associated with favorable prognosis in ovarian cancer**. *Proc Natl Acad Sci U S A* 2005, **102**(51):18538-18543.
51. Shen Z, Zhou S, Wang Y, Li RL, Zhong C, Liang C, Sun Y: **Higher intratumoral infiltrated Foxp3+ Treg numbers and Foxp3+/CD8+ ratio are associated with adverse prognosis in resectable gastric cancer**. *J Cancer Res Clin Oncol* 2010, **136**(10):1585-1595.
52. Hanks BA, Holtzhausen A, Evans KS, Jamieson R, Gimpel P, Campbell OM, Hector-Greene M, Sun L, Tewari A, George A *et al*: **Type III TGF-beta receptor downregulation generates an immunotolerant tumor microenvironment**. *J Clin Invest* 2013, **123**(9):3925-3940.

53. Yang P, Li QJ, Feng Y, Zhang Y, Markowitz GJ, Ning S, Deng Y, Zhao J, Jiang S, Yuan Y *et al*: **TGF-beta-miR-34a-CCL22 signaling-induced Treg cell recruitment promotes venous metastases of HBV-positive hepatocellular carcinoma**. *Cancer Cell* 2012, **22**(3):291-303.
54. Miyashita M, Sasano H, Tamaki K, Hirakawa H, Takahashi Y, Nakagawa S, Watanabe G, Tada H, Suzuki A, Ohuchi N *et al*: **Prognostic significance of tumor-infiltrating CD8+ and FOXP3+ lymphocytes in residual tumors and alterations in these parameters after neoadjuvant chemotherapy in triple-negative breast cancer: a retrospective multicenter study**. *Breast Cancer Res* 2015, **17**:124.
55. Meslin F, Thiery J, Richon C, Jalil A, Chouaib S: **Granzyme B-induced cell death involves induction of p53 tumor suppressor gene and its activation in tumor target cells**. *J Biol Chem* 2007, **282**(45):32991-32999.
56. De La Rochere P, Guil-Luna S, Decaudin D, Azar G, Sidhu SS, Piaggio E: **Humanized Mice for the Study of Immuno-Oncology**. *Trends Immunol* 2018, **39**(9):748-763.

Tables

Table 1. Time-dependent tumor volume with human PBMCs and/or TASO treatment

Group	Day 10	Day 12	Day 14	Day 16	Day 18
Tumor only	218.91 ± 28.36	309.46 ± 24.48	378.25 ± 66.93	479.28 ± 57.88	539.90 ± 56.84
PBMC+Vehicle	190.10 ± 43.24	223.05 ± 54.37 ##	270.91 ± 68.99 #	274.31 ± 104.48 ##	172.76 ± 34.28 ##
PBMC+TASO (16 mg/kg)	157.96 ± 31.43 *	139.27 ± 26.88 **	142.66 ± 38.10 **	145.75 ± 48.78 **	95.20 ± 33.01 *
PBMC+ TASO (32 mg/kg)	118.74 ± 40.43 **	136.03 ± 32.78 **	102.79 ± 24.15 **	90.37 ± 58.74 **	58.74 ± 35.08 **

Values were expressed as mean±S.D. of data obtained from five mice. # p<0.05 and ## p<0.01 vs. Tumor only. * p<0.05 and ** p<0.01 vs. PBMC+Vehicle (Dunnett's test).

Figures

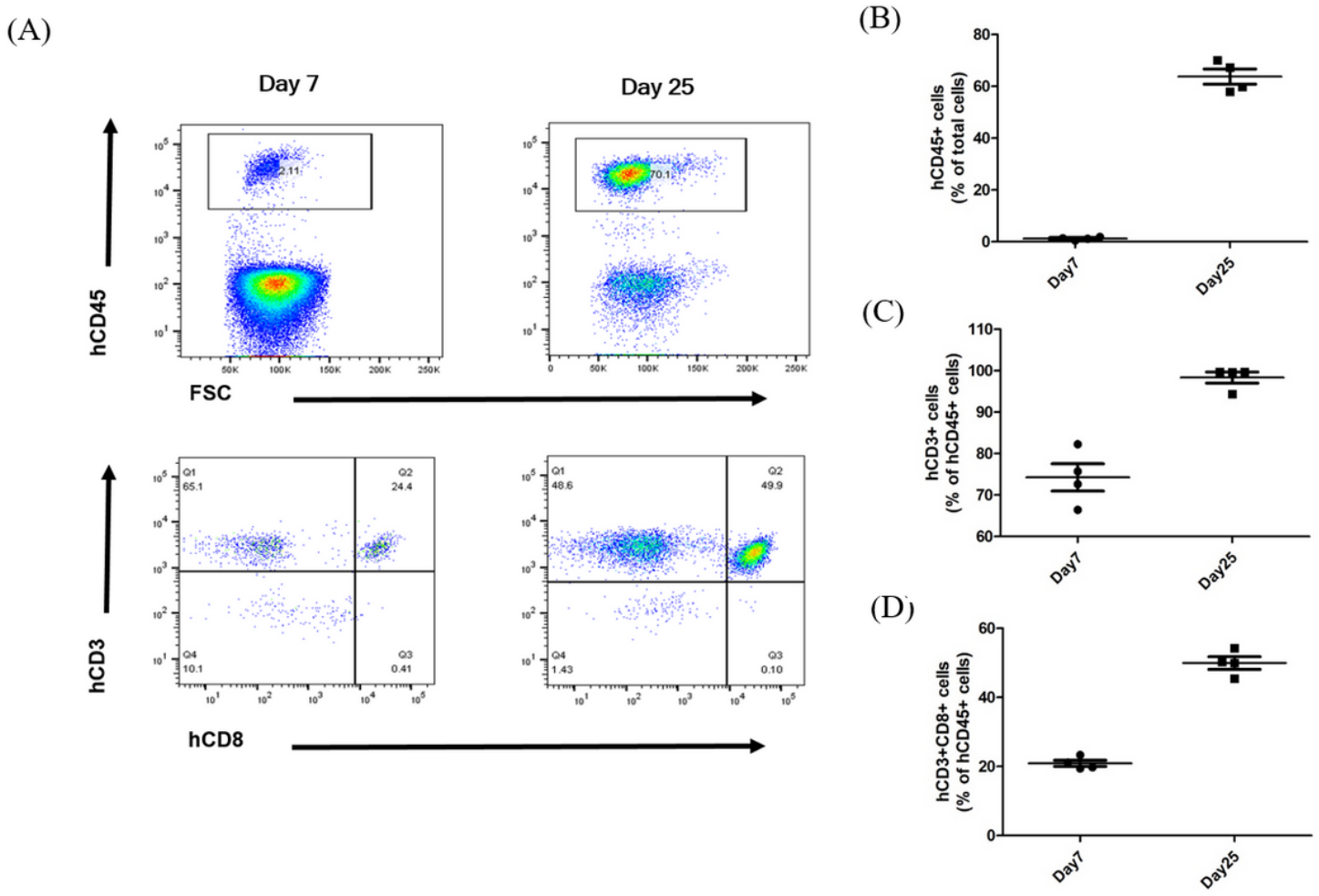

Figure 1

Generation of huPBL NSG mice (Preliminary experiment). Human CD3+ T cell dominant humanized mouse model is established by engrafting human PBMCs into NSG mouse. Subpopulations of human immune cells were measured by FACS analysis at days 7 and 25 after transplantation of human PBMCs into NSG mice. (A) Flow cytometry plots of human CD45+ cells in total gated cells, human T cells (hCD3+ cells) and human cytotoxic T cells (hCD3+CD8+ cells) in human CD45+-gated population. Flow cytometry data shows the percentage of (B) human CD45+ cells, and the percentage of (C) human CD3+ cells and (D) human CD3+CD8+ cells of the human CD45+ cells in blood (n=4).

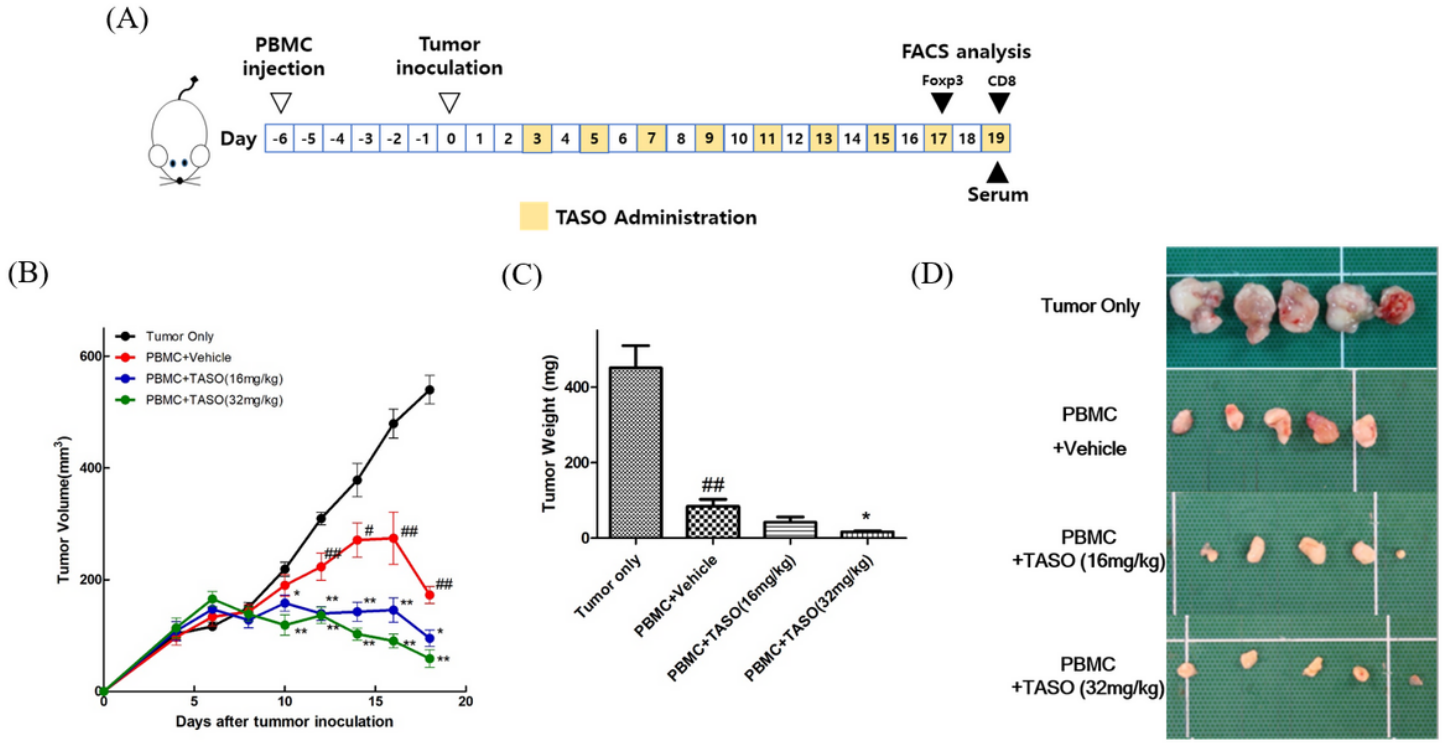

Figure 2

Effects of TGF-β2 inhibition by TASO on tumor growth in humanized mice. Tumor regression is accelerated by TASO administration in MDA-MB-231 xenografted huPBL NSG mice. (A) Experimental scheme for in vivo experiment. (B) Tumor volumes were measured by caliper every alternate day from day 4, and calculated using the formula (length) × (width)2/2. (C) Tumor weights and (D) corresponding images of tumor were measured at study termination (day 19 after tumor inoculation). The results are expressed as mean ± S.E.M. obtained from 5 mice. ## p<0.01 vs. Tumor only; * p<0.05 and ** p<0.01 vs. PBMC + vehicle (Dunnett's test).

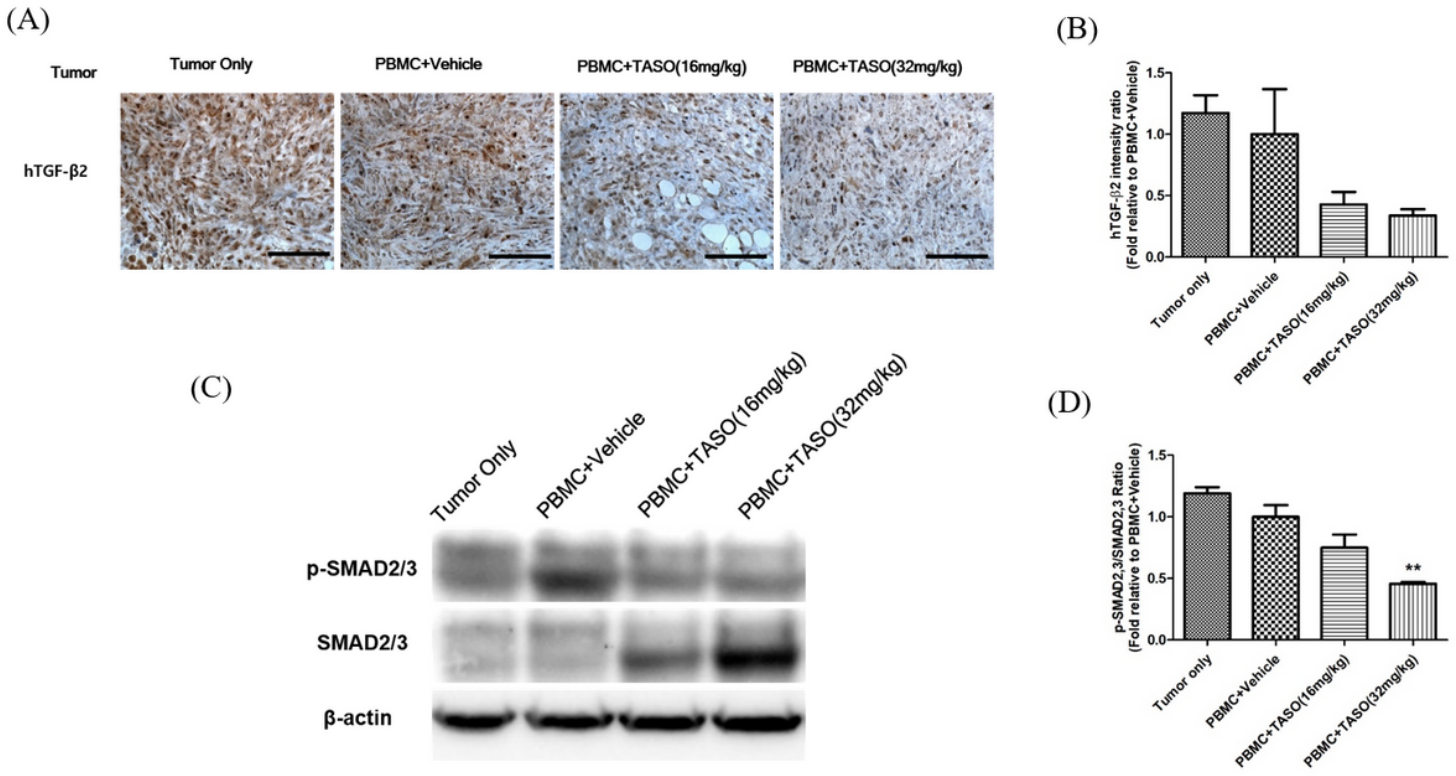

Figure 3

Effects of TASO on TGF-β2 production and TGF-β signaling in tumor. TGF-β2 synthesis and TGF-β downstream signaling in tumor are inhibited by TASO administration. Human TGF-β2 production in tumor was measured by IHC staining. (A) representative images and (B) its relative intensity were observed. TGF-β signaling was measured by western blot analysis of p-SMAD2/3 and SMAD2/3 in the tumor. (C) Representative band images of proteins and (D) the relative intensity of p-SMAD2/3 levels to SMAD 2/3 levels are presented. The results are expressed as mean ± S.E.M. ** $p<0.01$ vs. PBMC + vehicle (Dunnett's test). Each image is representative of 4-5 mice per group. Bar = 100 μm.

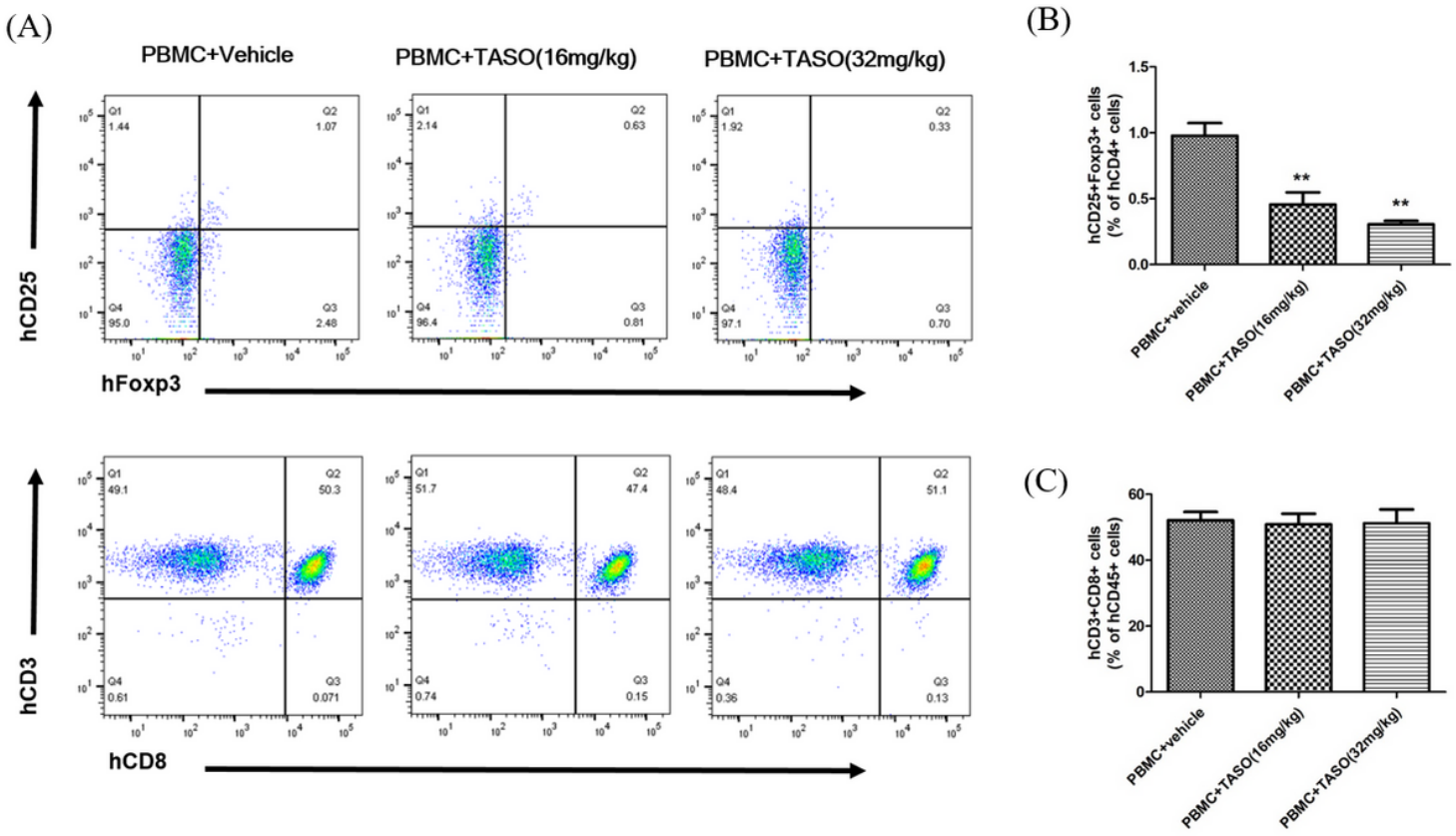

Figure 4

Effects of TGF-β2 inhibition by TASO on reconstitution of human T cells in blood. The subpopulation of Tregs is regulated by TGF-β2 inhibition in blood. Subpopulations of human Tregs and CD8+ T cells in peripheral blood were measured by FACS analysis on days 17 and 19 after tumor inoculation, respectively. (A) The flow cytometry plots of human Tregs (hCD25+Foxp3+ cells) in human CD4+-gated population, and human cytotoxic T cells (hCD3+CD8+ cells) in human CD45+-gated population, are presented. Flow cytometry data showing the percentage of (B) human Tregs (hCD25+Foxp3+ cells) among human CD4+ cells, and (C) human cytotoxic T cells (hCD3+CD8+ cells) among the human CD45+ cells in blood were measured. The results are expressed as mean ± S.E.M. obtained from 5 mice. ** $p<0.01$ vs. PBMC + vehicle (Dunnett's test).

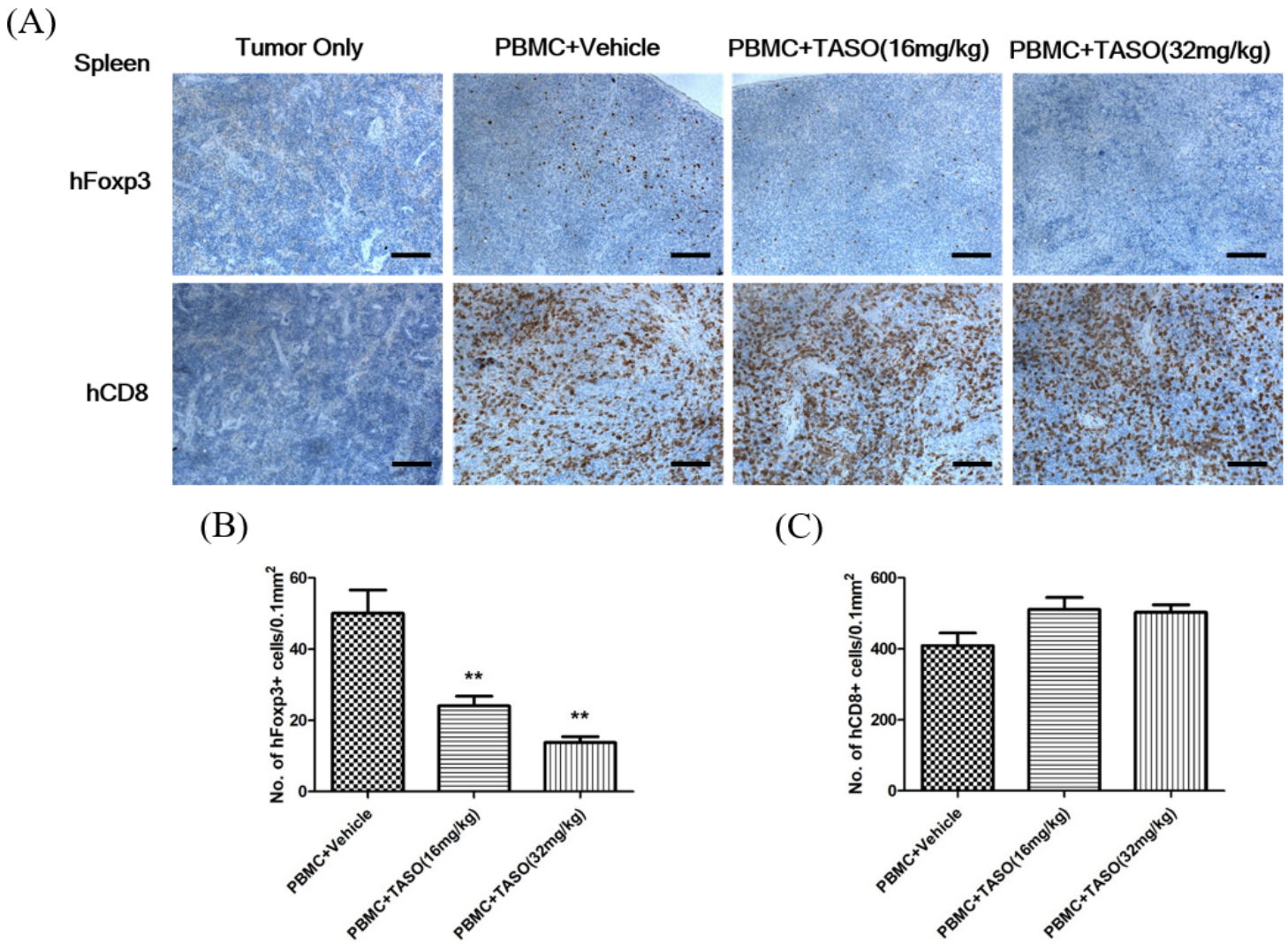

Figure 5

Effects of TGF-β2 inhibition by TASO on recruitment of human T cells in spleen. Subpopulation of Tregs is regulated by TGF-β2 inhibition in spleen. (A) Recruitment of human T cells in spleen was measured by IHC staining against human Foxp3 and human CD8. The human Foxp3 positive cells (B) and human CD8+ cells (C) were counted, and the density of cells (no. of 0.1 mm2) for phenotype of Tregs and cytotoxic T cells was determined, respectively. The results are expressed as mean ± S.E.M. obtained from 5 mice. ** $p<0.01$ vs. PBMC + vehicle (Dunnett's test). Bar = 100 μm.

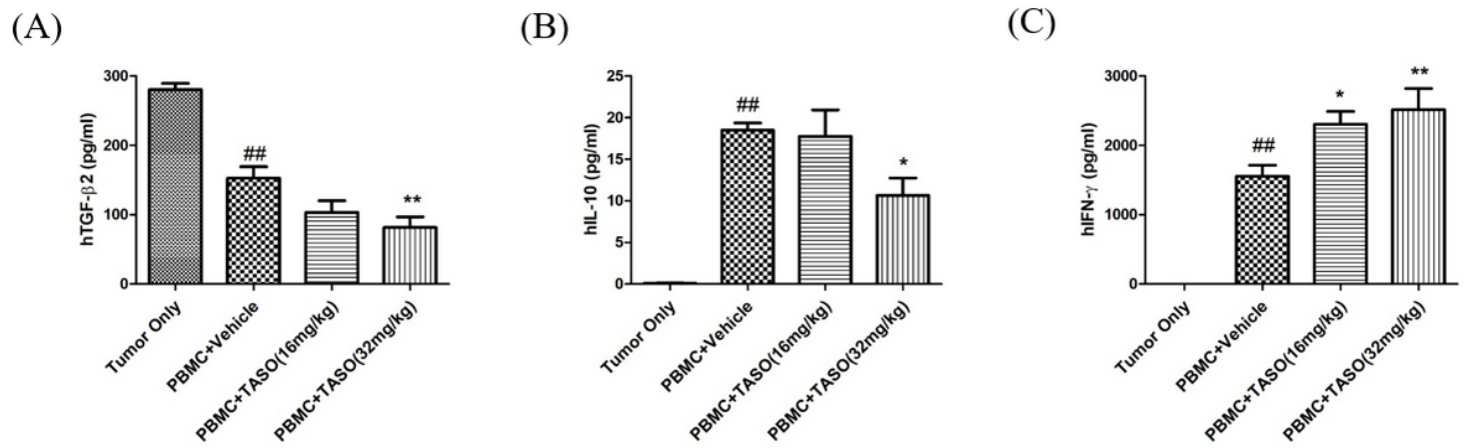

Figure 6

Effects of TGF-β2 inhibition by TASO on changes in human cytokine levels in huPBL NSG mice. Human cytokine levels are altered by TGF-β2 inhibition in huPBL NSG mice. Mouse sera were collected and assayed for the presence of (A) human TGF-β2, (B) human IL-10, and (C) human IFN-γ. The results are expressed as mean ± S.E.M. obtained from 5 mice. ## p<0.01 vs. Tumor only. * p<0.05 and ** p<0.01 vs. PBMC + vehicle (Dunnett's test).

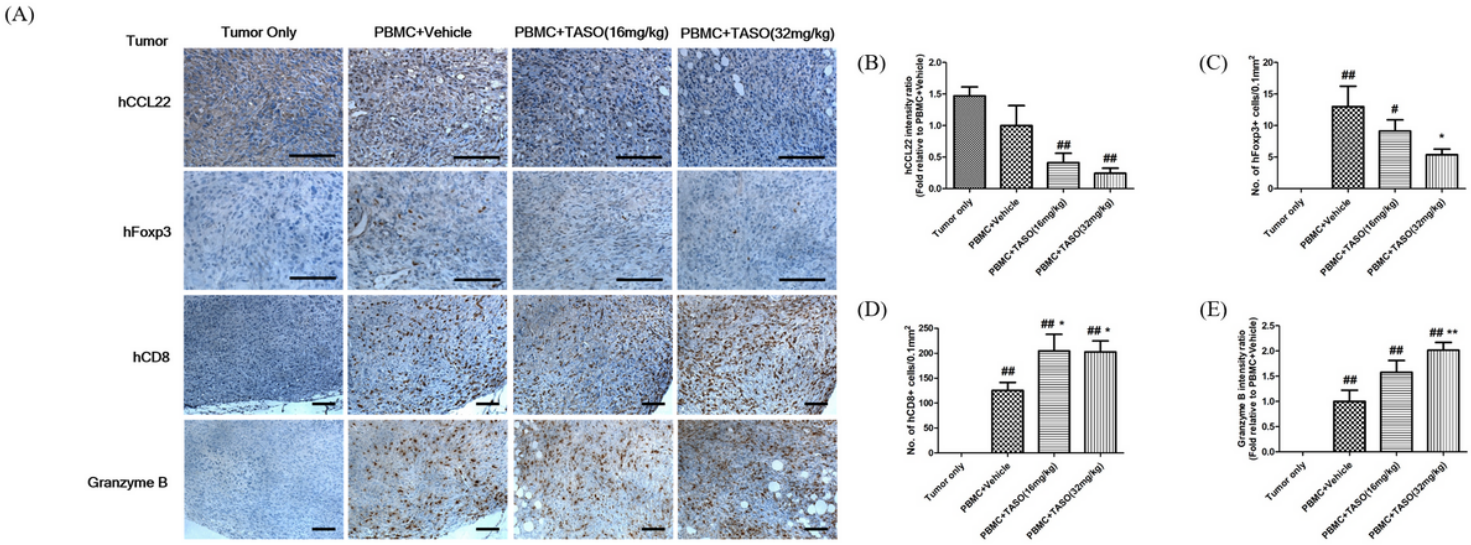

Figure 7

Effects of TGF-β2 inhibition by TASO on infiltration of human T cells into tumors and their activation. Infiltration and activation of human T cells in tumors are regulated by TGF-β2 inhibition. Infiltration and activation of human T cells in the tumor were measured by IHC staining against human CCL22, human Foxp3, human CD8, and granzyme B. (A) Each image is representative of 4-5 mice per group. The human Foxp3 positive cells (C) and human CD8+ cells (D) in tumor were counted, and the density of cells (no. of 0.1 mm2) for phenotype of Tregs and cytotoxic T cells was determined, respectively. Relative intensity of

(B) human CCL22 and (E) granzyme B were measured. # $p<0.05$ and ## $p<0.01$ vs. Tumor only. * $p<0.05$ and ** $p<0.01$ vs. PBMC + vehicle (Dunnett's test). Bar = 100 μm.